

DOI: <https://doi.org/10.15407/rpra29.01.068>  
UDC 537.874

A.A. Shmat'ko<sup>1</sup> and E.N. Odarenko<sup>2</sup>

<sup>1</sup>V.N. Karazin Kharkiv National University  
4, Svobody Sq., Kharkiv, 61022, Ukraine  
E-mail: sh47@ukr.net

<sup>2</sup>Kharkiv National University of Radio Electronics  
14, Nauki Ave., Kharkiv, 61166, Ukraine  
E-mail: yevhen.odarenko@nure.ua

## THE NARROW-BAND FILTER BASED ON A MAGNETOPHOTONIC CRYSTAL INVOLVING LAYERS WITH HYPERBOLIC DISPERSION LAWS

---

**Subject and Purpose.** Narrow-band filters are among the basic components of modern communication systems, instruments for spectroscopy, high-sensitivity sensors, etc. Photonic crystal structures open up broad possibilities for creating compact-sized, narrow-band filters in the optical and terahertz ranges. Tuning of spectral characteristics of photonic crystal filters is usually carried out through introduction of certain elements into their structure that are sensitive to external electric and magnetic fields. This work has been aimed at investigating electrodynamic characteristics of one-dimensional magnetophotonic crystals with structural layers characterized by "hyperbolic" dispersion, and suggesting a multichannel, narrow-band filter on their base.

**Methods and Methodology.** The dispersion equation for excitations in an infinite magnetophotonic crystal has been obtained within the framework of the Floquet-Bloch theory, with the use of fundamental solutions of Hill's equation. The transfer matrix approach has been used to obtain an analytical expression for the transmission coefficient.

**Results.** The band diagram of the one-dimensional magnetophotonic crystal has been analyzed for the case where one of the layers on the structure's spatial period is characterized by a hyperbolic dispersion law. The areas of existence of surface wave regimes have been found for such layers for the case of normal incidence of the wave upon the finite-seized magnetophotonic crystal. Frequency dependences of the transmission coefficient are characterized by a set of high-Q resonant peaks relating to Fabry-Perot resonances in a periodic structure of finite length.

**Conclusions.** Application of a finite-seized, one-dimensional magnetophotonic crystal is considered as of a means for achieving multichannel optical filtering and formation of a frequency comb. Expressions for the dispersion equation and transmission coefficient have been obtained within the framework of the Floquet-Bloch theory and with the use of the transfer matrix. The feasibility of surface mode excitation has been shown for gyrotropic layers of the periodic structure characterized by a hyperbolic dispersion law, for the case of normal incidence upon the magnetophotonic crystal. The spectral response of the filter contains narrow-band peaks with a high transmission efficiency. By increasing the number of the structure's periods it is possible to form a frequency comb, which effect can be useful for applications in metrology and modern optical communication systems.

**Keywords:** magnetophotonic crystals, hyperbolic media, narrow-band filtering, frequency comb, dispersion characteristics, surface wave modes.

---

Citation: Shmat'ko, A.A., and Odarenko, E.N., 2024. The narrow-band filter based on a magnetophotonic crystal involving layers with hyperbolic dispersion laws. *Radio Phys. Radio Astron.*, 29(1), pp. 68–75. <https://doi.org/10.15407/rpra29.01.068>

Цитування: Шматько О.О., Одаренко Є.М. Вузькосмуговий фільтр на основі магнітофотонного кристала, що містить шари з гіперболічним законом дисперсії. *Радіофізика і радіоастрономія*. 2024. Т. 29, № 1. С. 68–75. <https://doi.org/10.15407/rpra29.01.068>

© Publisher ПН "Академперіодика" of the NAS of Ukraine, 2024. This is an open access article under the CC BY-NC-ND license (<https://creativecommons.org/licenses/by-nc-nd/4.0/>)

© Видавець ВД «Академперіодика» НАН України, 2024. Статтю опубліковано відповідно до умов відкритого доступу за ліцензією CC BY-NC-ND (<https://creativecommons.org/licenses/by-nc-nd/4.0/>)

## Introduction

Photonic crystals which are inherently artificial dielectrics characterized by periodic modulation of their material parameters are widely used for controlling propagation characteristics of electromagnetic excitations [1–3]. This functionality of photonic crystals owes to the presence of a photonic band where the propagation is prohibited. The omnidirectional band gap is the key property to allow localization of electro-magnetic energy within defects of periodicity.

Both dielectric and metallic photonic crystal structures can provide possibilities for creating a broad range of devices that permit controlling a variety of characteristics of optical or microwave signals [4–6]. Photonic crystal waveguides and resonators can be relatively easily implemented in various integrated systems [7–12]. One-dimensional photonic crystals are the simplest version of periodic structures, both from the point of manufacturing technologies and theoretical study of their performance characteristics.

The one-dimensional magnetophotonic crystals (MPhCs) contain layers of materials that are sensitive to an external magnetic field [13–15]. Thus, it is possible to control the characteristics of such structures and create various tunable devices exploiting their properties, such as waveguides, resonators, filters, circulators, insulators, etc. [16–19]. The tensorial nature of their permittivity and magnetic permeability is a characteristic feature of magneto-optical media. In addition, the one-dimensional photonic crystals allow formation of materials with unusual electrodynamic properties (metamaterials). A promising direction of such studies is represented by the so called hyperbolic media for which isofrequency surfaces in dispersion law representations are hyperboloids [20–23]. Therefore, such materials provide support for large wave numbers, which opens up possibilities for a variety of practical applications.

The combined use of photonic crystal waveguides and resonators provides a basis for implementing filtering functions. Photonic crystal resonators demonstrating high Q-factors open up possibilities for narrow-band signal filtering, which is especially important for telecommunication systems, sensors, spectroscopy, etc. [24–33]. The waveguides and resonators required for the purpose are implemented

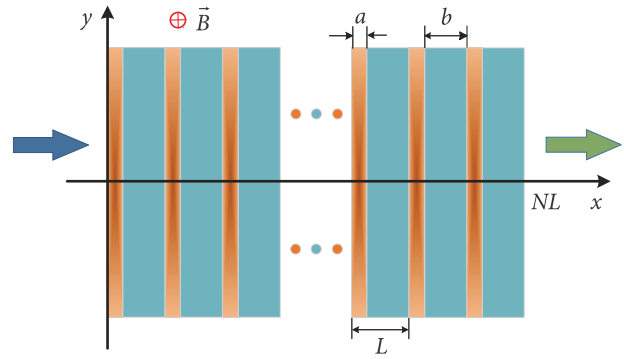


Fig. 1. Schematic of the 1D magnetophotonic crystal

through formation of linear and local periodicity defects in the photonic crystals. The filters based on one-dimensional photonic crystals usually involve the resonators that are formed by a defective layer surrounded on both sides by multilayered periodic structures [34–36].

In this paper, we propose a different approach to the implementation of a multichannel, narrow-band filter based on the one-dimensional photonic crystal. The filter is based on a finite-sized one-dimensional magnetophotonic crystal involving no periodicity defects. The necessary spectral characteristics of the filter are provided by the presence of layers with hyperbolic dispersion laws, which are alternated with dielectric layers. The surface wave regimes realizable in the "hyperbolic" layers of the structure have allowed obtaining narrow-band transmission zones characterized by a high transmission coefficient.

## 1. Basic theoretical relations

Figure 1 shows a schematic of the one-dimensional MPhC under consideration, within an appropriate coordinate system. The periodic structure consists of an alternating sequence of gyrotropic and dielectric layers (designated by numbers 1 and 2, respectively). The permittivity of a "hyperbolic" gyrotropic layer of thickness  $a$  is described by the tensor

$$\leftrightarrow \varepsilon_1(x) = \begin{pmatrix} \varepsilon_{xx} & -i\varepsilon_a & 0 \\ i\varepsilon_a & \varepsilon_{yy} & 0 \\ 0 & 0 & \varepsilon_{zz} \end{pmatrix}.$$

The isotropic dielectric layers are characterized by thickness  $b$  and permittivity  $\varepsilon_2 = 12$  (also,  $\mu_2 = \mu_1 = 1$ ). Within the framework of a two-dimensional approximation, the two polarizations of

the radiation of interest can be considered separately. As a result, the Helmholtz equations for the TE-polarized ( $H_z$ -polarized) wave modes existing in layers 1 and 2 of the periodic structure can be written as

$$\frac{1}{\varepsilon_{yy}} \frac{\partial^2 H_{z1}}{\partial x^2} + \frac{1}{\varepsilon_{xx}} \frac{\partial^2 H_{z1}}{\partial y^2} + k^2 \mu_1 \varepsilon_{\perp} H_{z1} = 0,$$

$$\frac{\partial^2 H_{z2}}{\partial x^2} + \frac{\partial^2 H_{z2}}{\partial y^2} + k^2 \mu_2 \varepsilon_2 H_{z2} = 0,$$

where

$$k = \frac{\omega}{c}, \quad \varepsilon_{\perp xy} = \varepsilon_{xx} \left( 1 - \frac{\varepsilon_a^2}{\varepsilon_{xx} \varepsilon_{yy}} \right) = \varepsilon_{xx} \varepsilon_{\perp},$$

$$\varepsilon_{xx} = \varepsilon_{\infty} \left( 1 - \frac{\omega_p^2}{\omega^2 - \omega_c^2} \right), \quad \varepsilon_{yy} = \varepsilon_{zz} = \varepsilon_{\infty} \left( 1 - \frac{\omega_p^2}{\omega^2} \right),$$

and  $\varepsilon_a = -\frac{\omega_c \omega_p^2}{\omega(\omega^2 - \omega_c^2)}$ ,  $\omega_c = \frac{|e|}{m_0} B_0$ ,

$$\omega_p = \left( \frac{e^2 N_0}{m_0^*} \right)^{1/2}.$$

Here  $\varepsilon_{\infty} = 12$  is the high frequency permittivity;  $e$  and  $m_0$  are the charge and mass of the electron;  $m_0^*$  is the electron's effective mass;  $\omega_c$  is the gyromagnetic frequency;  $B_0$  is the external magnetostatic field induction;  $N_0$  is the electron concentration, and  $\omega_p$  is the plasma frequency of the gyrotropic layer.

The magnitudes of the tangential electric component  $E_y$  taken in the periodic structure's layers can be expressed via the  $H_z$  component as

$$E_{y1} = \frac{1}{ik\varepsilon_{\perp xy}} \left( \frac{\partial H_{z1}}{\partial x} - \beta \frac{\varepsilon_a}{\varepsilon_{xx}} H_{z1} \right) e^{i\beta y},$$

$$E_{y2} = \frac{1}{ik\varepsilon_2} \frac{\partial H_{z2}}{\partial x} e^{i\beta y},$$

where  $\beta$  is the propagation constant.

Similar relations for the other (namely,  $E_z$ ) polarization can be obtained through the use of the permutative duality principle.

The modal equation for TE waves in an infinite MPhC with gyrotropic layers can be derived, based on the Floquet-Bloch method. By applying the representation  $H_z = X(x)e^{i\beta y}$  it is possible to reduce the Helmholtz equations to Hill's equations like

$$\frac{\partial^2 X(x)}{\partial x^2} + \xi_j^2(x) X(x) = 0, \quad (1)$$

where the subscript  $j = 1, 2$  denotes the layer number and  $\xi_j$  is the transverse wave number in layer  $j$ , so

$$\xi_1 = \sqrt{k^2 \mu_1 \varepsilon_{yy} \varepsilon_{\perp} - \frac{\varepsilon_{yy}}{\varepsilon_{xx}} \beta^2}, \quad \xi_2 = \sqrt{k^2 \mu_2 \varepsilon_2 - \beta^2}.$$

Any solution to Eq. (1) can be expressed as a linear combination of the two fundamental solutions  $\psi_1(x)$  and  $\psi_2(x)$  of the Hill equation,

$$X(x) = A\psi_1(x) + B\psi_2(x).$$

Analytical expressions for the functions  $\psi_1(x)$  and  $\psi_2(x)$  for each layer on the structure's period can be obtained as solutions of the third boundary-value problem [23],

$$\psi_1(x) = \begin{cases} \cos \xi_1 x + \beta \frac{\varepsilon_a}{\varepsilon_{xx}} \frac{\sin \xi_1 x}{\xi_1}, & 0 < x < a, \\ A \cos \xi_2(x-a) - B \frac{\sin \xi_2(x-a)}{\xi_2}, & a < x < L; \end{cases} \quad (2)$$

$$\psi_2(x) = \begin{cases} \varepsilon_{\perp xy} \frac{\sin \xi_1 x}{\xi_1}, & 0 < x < a, \\ C \cos \xi_2(x-a) + D \frac{\sin \xi_2(x-a)}{\xi_2}, & a < x < L, \end{cases} \quad (3)$$

$$\text{with } A = \left( \cos \xi_1 a + \beta \frac{\varepsilon_a}{\varepsilon_{xx}} \frac{\sin \xi_1 a}{\xi_1} \right),$$

$$B = \frac{\varepsilon_2}{\varepsilon_{\perp xy}} \left[ \xi_1 \sin \xi_1 a + \left( \beta \frac{\varepsilon_a}{\varepsilon_{xx}} \right)^2 \frac{\sin \xi_1 a}{\xi_1} \right], \text{ and}$$

$$C = \varepsilon_{\perp xy} \frac{\sin \xi_1 a}{\xi_1}, \quad D = \varepsilon_2 \left[ \cos \xi_1 a - \beta \frac{\varepsilon_a}{\varepsilon_{xx}} \frac{\sin \xi_1 a}{\xi_1} \right].$$

Application of the Floquet theorem results in a set of homogeneous equations for the function  $X(x)$  formulated at boundaries of structural layers,

$$\rho X_1(0) = X_2(L),$$

$$\rho \frac{1}{\varepsilon_{\perp xy}} \left( \frac{\partial X_1(0)}{\partial x} - \beta \frac{\varepsilon_a}{\varepsilon_{xx}} X_1(0) \right) = \frac{1}{\varepsilon_2} \frac{\partial X_2(L)}{\partial x},$$

where  $\rho$  is the Floquet factor which satisfies the characteristic equation:

$$\rho^2 - 2A_H \rho + 1 = 0. \quad (4)$$

Here  $A_H = \psi_1(L) + \psi_2'(L) / \varepsilon_2$  is Hill's discriminant [37]. By solving Eq. (4) with account of expres-

sions (2) and (3) we arrive at a dispersion equation for Bloch's wave number  $K$  for the infinite-seized MPnC,

$$\begin{aligned} \cos KL = \frac{A_H}{2} = \cos \xi_1 a \cos \xi_2 b - \\ - \frac{1}{2} \left[ \frac{\epsilon_{\perp xy} \xi_2}{\epsilon_2 \xi_1} + \frac{\epsilon_2}{\epsilon_{\perp xy}} \left( \frac{\xi_1}{\xi_2} + \frac{\beta^2}{\xi_1 \xi_2} \left( \frac{\epsilon_a}{\epsilon_{xx}} \right)^2 \right) \right] \times \\ \times \sin \xi_1 a \sin \xi_2 b. \end{aligned} \quad (5)$$

It is worth noting that the dispersion equation Eq. (5) is the same as the equation obtained in paper [38] by the well-known transfer matrix method.

Upon applying the proper boundary conditions to the fundamental solutions we obtain a matrix equation relative tangential field components at the boundaries of the finite-sized photonic crystal containing  $N$  periods,

$$\begin{pmatrix} H_z(NL) \\ E_y(NL) \end{pmatrix} = W^N \begin{pmatrix} H_z(0) \\ E_y(0) \end{pmatrix}, \quad (6)$$

where

$$W = \begin{pmatrix} W_{11} & W_{12} \\ W_{21} & W_{22} \end{pmatrix} = \begin{pmatrix} \psi_1(L) & ik\psi_2(L) \\ \frac{\psi_1'(L)}{ik\epsilon_2} & \frac{\psi_2'(L)}{\epsilon_2} \end{pmatrix}.$$

Proceeding from Eq. (6) and the relevant boundary conditions one can write down the matrix equation allowing to find the reflection and transmission coefficients, specifically

$$T \begin{pmatrix} 1 \\ \frac{\xi_0}{k} \end{pmatrix} = \begin{pmatrix} W_{11} & W_{12} \\ W_{21} & W_{22} \end{pmatrix}^N \begin{pmatrix} R \\ \frac{\xi_0}{k} (1-R) \end{pmatrix},$$

with  $\xi_0 = \sqrt{k^2 - \beta^2}$ . Then the transmission coefficient of the structure can be written as [39]

$$\begin{aligned} T = & \left[ 1 + \sin^2 NKL \times \right. \\ & \left. \times \left( \left( \frac{1}{2 \sin KL} \right)^2 \left| \left( \xi_0 \psi_2(L) - \frac{\psi_1'(L)}{\xi_0 \epsilon_2} \right) \right|^2 - 1 \right) \right]^{-1}. \end{aligned} \quad (7)$$

## 2. Analysis of results

First we consider dispersion properties of the gyrotropic medium which forms up one of the layers over the structure's period. The dispersion relation for an infinite gyrotropic medium can be represented as

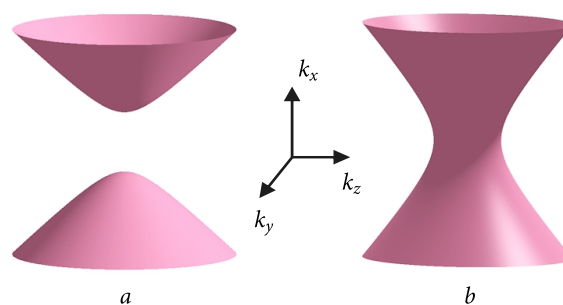


Fig. 2. Isofrequency surfaces for (a) Type I hyperbolic medium, (b) Type II hyperbolic medium

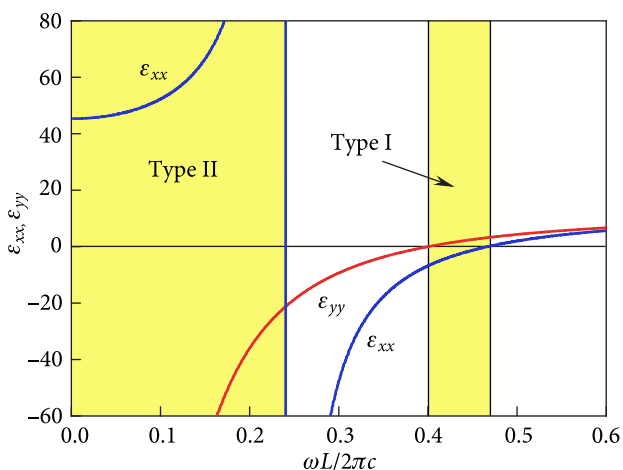


Fig. 3. Diagonal components of the permittivity tensor in dependence on the normalized frequency

an equation of ellipse in the space of wave numbers, specifically

$$\frac{k_x^2}{\epsilon_{yy}} + \frac{k_y^2}{\epsilon_{xx}} = k^2 \mu_1 \epsilon_{\perp} = k^2 \mu_1 \left( 1 - \frac{\epsilon_a^2}{\epsilon_{xx} \epsilon_{yy}} \right). \quad (8)$$

Meanwhile, if we assume one of the diagonal components of the permittivity tensor ( $\epsilon_{xx}$  or  $\epsilon_{yy}$ ) to be a negative value, then we arrive at the equation of a hyperbola. Shown in Fig. 2 are hyperboloidal isofrequency surfaces of two kinds, corresponding to different types of "hyperbolic" media in the general case of a three-dimensional wave number space, namely Type I (dual-sheet hyperboloid) and Type II (single-sheet hyperboloid) [20]. Equation (8) describes traces of these hyperboloids in the  $k_x k_y$ -plane.

The unique physical characteristics of "hyperbolic" media are conditioned by frequency dependences of the permittivity tensor components. Fig. 3 shows these dependencies for the diagonal components  $\epsilon_{xx}$  and  $\epsilon_{yy}$  with parameters like  $\omega_p = 0.4$

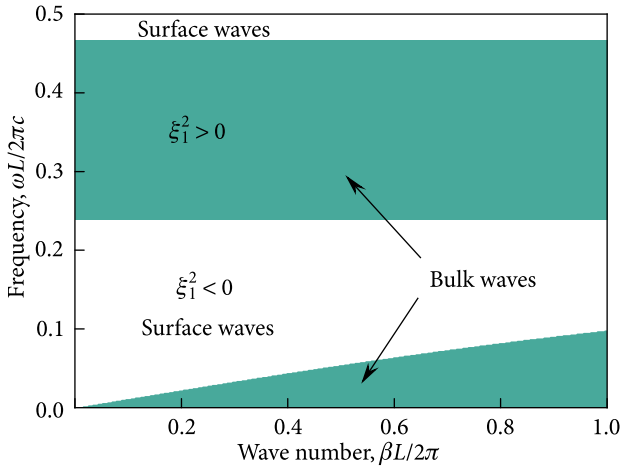


Fig. 4. Dispersion diagram typical of "hyperbolic" gyrotropic media

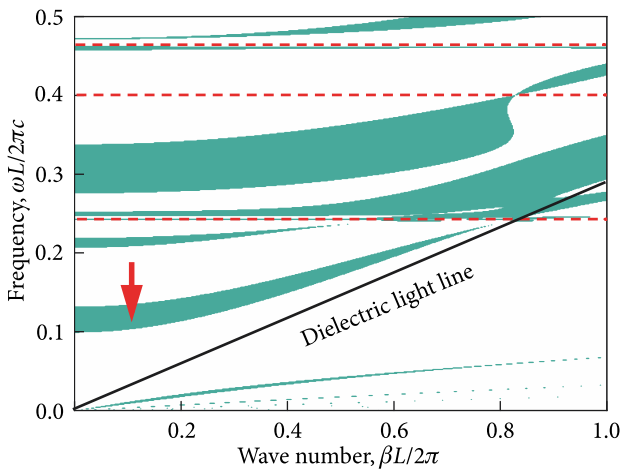


Fig. 5. Dispersion diagram of the 1D magnetophotonic crystal containing hyperbolic gyrotropic layers

and  $\omega_c = 0.24$ . The shaded areas indicate different types of hyperbolicity. The tensor components  $\epsilon_{xx}$  and  $\epsilon_{yy}$  can be seen to assume magnitudes of both positive and negative signs over the frequency ranges under consideration. The shaded and the unshaded areas in Fig. 4 represent real and purely imaginary values of the transverse wave number  $\xi_1$ , respectively, corresponding to transmission and forbidden zones in an infinite "hyperbolic" medium. Naturally, these areas also identify existence conditions for bulk and surface wave modes in the hyperbolic layers of the MPhC under consideration.

It should be noted that we have obtained surface wave excitation conditions for the case of normal incidence ( $\beta = 0$ ) of the primary wave on the hyperbolic medium. The result is unusual, since in a pu-

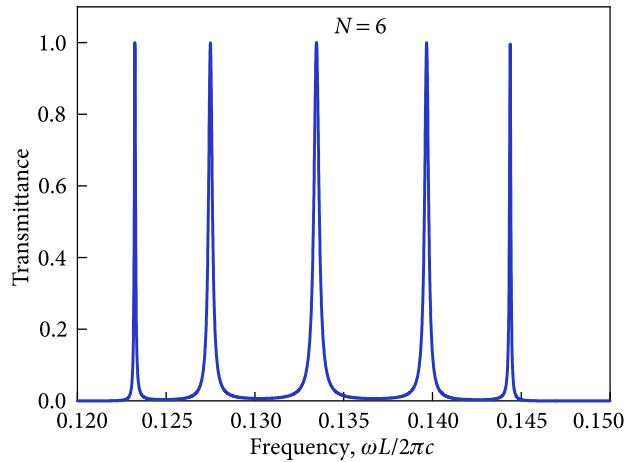


Fig. 6. Transmission coefficient of a magnetophotonic crystal as a function of normalized frequency ( $N = 6$ )

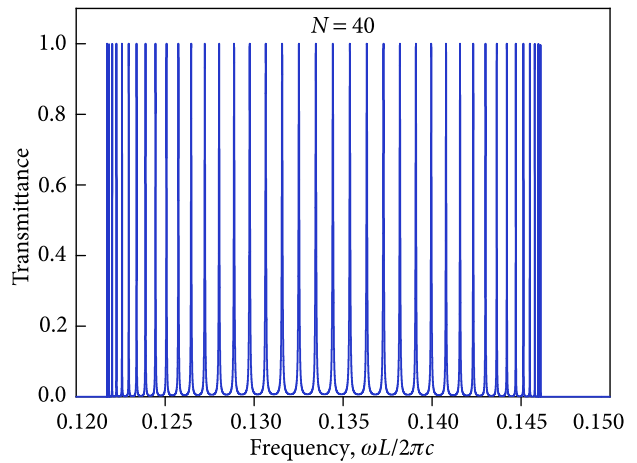


Fig. 7. Transmission coefficient of a magnetophotonic crystal as a function of normalized frequency ( $N = 40$ )

rely dielectric medium surface wave modes can be excited solely under oblique incidence conditions [40–43].

Analysis of the bulk and surface wave modes of the MPhC requires solution of the dispersion Eq. (5). The dispersion diagram in Fig. 5 shows the results for parameter values  $a = 0.1L$ ;  $\epsilon_\infty = 12$ ;  $\omega_p = 0.4$ ;  $\omega_c = 0.24$ . The shaded areas indicate transmission zones of the MPhC, while the unshaded areas correspond to forbidden zones. The dashed lines show boundaries of regions supporting the "hyperbolic" regimes. Evidently, the hyperbolicity of the MPhC layers results in appearance of transmission zones for surface wave modes in gyrotropic layers of "hyperbolic" kind. One of such zones is indicated by an arrow in Fig. 5. The oblique line in the Figure indi-

cates a light line for the dielectric layer of the MPhC. Thus, the transmission zones noted here correspond to surface wave modes in "hyperbolic" layers and bulk modes in dielectric ones.

Shown in Fig. 6 is the transmittance factor of a finite-seized MPhC containing six periods ( $N = 6$ ). The transmission coefficient Eq. (7) has been calculated for a frequency band corresponding to surface wave modes in "hyperbolic" layers. There are  $(N - 1)$  narrow transmission peaks separated by forbidden zones. The physical nature of a similar frequency dependence stems from Fabry-Perot resonances in bounded periodic structures [39]. The high Q-factors of these resonances allow developing multichannel, narrow passband filters for optical communication systems and other applications. Each transmission peak can be regarded as an individual transmission channel for the signals of interest. It should be noted that other frequency bands corresponding to surface wave modes in hyperbolic gyrotropic layers are characterized by the same spectral properties as shown in Fig. 6. Accordingly, these transmission bands can be used for narrow passband filtering as well.

As can be seen from the dispersion diagram of Fig. 5, increasing the incidence angle of radiation brings forth a blueward shift of the transmission band under investigation. Furthermore, the transmitted bandwidth gets changed too. This physical mechanism can provide for fine tuning of the filter's spectral characteristics.

Another way to adjust the filter characteristics is to change the "hyperbolic" layer's thickness  $a$  and the external magnetic induction  $B_0$ . The respective calculations show that an increase in the hyperbolic

layer's thickness leads to narrowing of the transmission band of the surface wave modes, up to their complete disappearance. Furthermore, changes of the structural layers' thicknesses can affect the isofrequency surfaces transformation [44]. By tuning the magnetic field it is possible to significantly change the dispersion diagram and vary locations of transmission zones for the bulk and surface wave modes.

It is well-known that the number of transmission peaks within the passbands is defined by the number of structural periods. Fig. 7 shows the transmittance of a MPhC involving 40 spatial periods ( $N = 40$ ). As appears, the spectral characteristic of the finite-seized MPhC represents in this case a flat-top frequency comb with almost uniform spacings.

Consequently, such periodic structures can also be used in optical frequency comb generation schemes suitable for many applications in metrology and optical communications systems.

## Conclusions

It has been shown that one-dimensional MPhCs containing "hyperbolic" gyrotropic layers can be used for multichannel filtering and formation of frequency combs. The frequency-domain performance characterized by high-Q resonances is achieved owing to existence of surface wave modes in the "hyperbolic" layers. An analytical expression for the transmission coefficient has been obtained within the framework of the Floquet-Bloch wave method and use of the transfer matrix technique. The frequency characteristics of the MPhC can be controlled by changing the angles of wave incidence, thickness of the "hyperbolic" layer and external magnetic induction.

## REFERENCES

1. Joannopoulos, J.D., Johnson, S.G., Winn, J.N., and Meade, R.D., 2008. *Photonic Crystals: Molding the Flow of Light*. Princeton University Press. 304 pp.
2. Prather, D.W., Sharkawy, A., Shi, S., Murakowski, J., and Schneider, G., 2009. *Photonic Crystals, Theory, Applications and Fabrication*. Wiley. 416 pp.
3. Sakoda, K., 2005. *Optical Properties of Photonic Crystals*. Springer-Verlag Berlin Heidelberg. 258 pp.
4. Gong, Q., and Hu, X., 2013. *Photonic Crystals. Principles and Applications*. Pan Stanford Publishing. 366 pp.
5. Skorobogatiy, M., and Yang, J., 2009. *Fundamentals of Photonic Crystal Guiding*. Cambridge University Press. 280 pp.
6. Ivzhenko, L.I., Odarenko, E.N., and Tarapov, S.I., 2016. Mechanically tunable wire medium metamaterial in the millimeter wave band. *Prog. Electromagn. Res. Lett.*, **64**, pp. 93–98. DOI: 10.2528/PIERL16090903
7. Krauss, T.F., 2003. Planar photonic crystal waveguide devices for integrated optics. *Phys. Stat. Sol.*, **197**(3), pp. 688–702. DOI: 10.1002/pssa.200303117
8. Ikeda, N., Sugimoto, Y., Tanaka, Y., Inoue, K., and Asakawa, K., 2005. Low propagation losses in single-line-defect photonic crystal waveguides on Ga-As membranes. *IEEE J. Sel. Areas Commun.*, **23**(7), pp. 1315–1320. DOI: 10.1109/JSAC.2005.851215
9. Englund, D., Ellis, B., Edwards, E., Sarmiento, T., Harris, J.S., Miller, D.A.B., and Vučković, J., 2009. Electrically controlled modulation in a photonic crystal nanocavity. *Opt. Express*, **18**, pp. 15409–15419. DOI: 10.1364/OE.17.015409

10. Stievater, T.H., Pruessner, M.W., Rabinovich, W.S., Park, D., Mahon, R., Kozak, D.A., Boos, J.B., Holmstrom, S.A., and Khurgin, J.B., 2015. Suspended photonic waveguide devices. *Appl. Opt.*, **54**(31), pp. F164–F173. DOI: 10.1364/AO.54.00F164
11. Akahane, Y., Asano, T., Song, B., and Noda, S., 2005. Fine-tuned high-Q photonic-crystal nanocavity. *Opt. Express*, **13**, pp. 1202–1214. DOI: 10.1364/OPEX.13.001202
12. Sashkova, Ya.V., and Odarenko, Ye.N., 2018. The modified Bragg waveguide with additional layers. *Telecommunications and Radio Engineering*, **77**(6), pp. 489–500. DOI: 10.1615/TelecomRadEng.v77.i6.20
13. Inoue, M., Fujikawa, R., Baryshev, A., Khanikaev, A., Lim, P.B., Uchida, H., Aktsipetrov, O., Fedyanin, A., Murzina, T., and Granovsky, A., 2006. Magnetophotonic crystals. *J. Phy. D: Appl. Phys.*, **39**, pp. 151–161. DOI: 10.1088/0022-3727/39/8/R01
14. Shmat'ko, A.A., Mizernik, V.N., and Odarenko, E.N., 2020. Floquet-Bloch waves in magnetophotonic crystals with transverse magnetic field. *Journal of Electromagnetic Waves and Applications*, **34**(12), pp. 1667–1679. DOI: 10.1080/09205071.2020.1780955
15. Shmat'ko, A.A., Odarenko, E.N., Mizernik, V.N., and Rokhmanova, T.N., 2017. Bragg reflection and transmission of light by one-dimensional gyrotropic magnetophotonic crystal. In: *2017 2nd Int. Conf. on Advanced Information and Communication Technologies (AICT)*. Lviv, Ukraine, 04–07 July 2017. P. 232–236. DOI: 10.1109/AICT.2017.8020108
16. Zhang, Y., Li, P., Chen, Y., and Han, Y., 2019. Four-channel THz wave routing switch based on magneto photonic crystals. *Optik*, **181**, pp. 134–139. DOI: 10.1016/j.ijleo.2018.12.032
17. Fei, H., Wu, J., Yang, Y., Liu, X., and Chen, Z., 2015. Magneto-optical isolators with flat-top responses based on one-dimensional magneto-photonic crystals. *Photonics Nanostruct.*, **17**, pp. 15–21. DOI: 10.1016/j.photonics.2015.10.001
18. Xu, B., Zhang, D., Zeng, X., Wang, Y., and Dong, Z., 2019. Magnetic photonic crystal circulator based on gradient changing width waveguide. *Optik*, **185**, pp. 132–137. DOI: 10.1016/j.ijleo.2019.03.054
19. Zeng, C., Wang, Z., and Xie, Y., 2019. Transmission characteristics of linearly polarized light in reflection-type one-dimensional magnetophotonic crystals. *Front. Optoelectron.*, **12**, pp. 365–371. DOI: 10.1007/s12200-019-0870-0
20. Ferrari, L., Wu, C., Lepage, D., Zhang, X., and Liu, Zh., 2015. Hyperbolic metamaterials and their applications. *Prog. Quantum Electron.*, **40**, pp. 1–40. DOI: 10.1016/j.pquantelec.2014.10.001
21. Mirmoosa, M.S., Kosulnikov, S.Yu., and Simovski, C.R., 2016. Magnetic hyperbolic metamaterial of high-index nanowires. *Phys. Rev. B*, **94**, 075138. DOI: 10.1103/PhysRevB.94.075138
22. Tuz, V.R., Fesenko, V.I., 2020. Magnetically induced topological transitions of hyperbolic dispersion in biaxial gyrotropic media. *J. Appl. Phys.*, **128**(1), 013107. DOI: 10.1063/5.0013546
23. Shmat'ko, A.A., Odarenko, E.N., and Mizernik, V.N., 2020. Hyperbolic magnetophotonic crystals with gyrotropic layers. Dispersion characteristics. In: *2020 IEEE Ukrainian Microwave Week (UkrMW)*. Kharkiv, Ukraine, 21–25 Sept. 2020. Vol. 4, pp. 1094–1098. DOI: 10.1109/UkrMW49653.2020.9252717
24. Fan, S., Wang, Z., Miller, D.A.B., Villeneuve, P.R., Haus, H.A., and Joannopoulos, J.D., 2002. Photonic crystal for communication applications. *Proc. SPIE*, **4870**, pp. 298–306. DOI: 10.1117/12.475546
25. Ghosh, R., Ghosh, K.K., and Chakraborty, R., 2013. Narrow band filter using 1D periodic structure with defects for DWDM systems. *Opt. Commun.*, **289**, pp. 75–80. DOI: 10.1016/j.optcom.2012.10.001
26. González, L.E., Segura-Gutierrez, L.M., Ordoñez, J.E., Zambrano, G., and Reina, J.H., 2022. A Multichannel Superconductor-Based Photonic Crystal Optical Filter Tunable in the Visible and Telecom Windows at Cryogenic Temperature. *Photonics*, **9**(7), pp. 485–497. DOI: 10.3390/photonics9070485
27. Dangi, M.M., Aghdam, A.M., Karimzadeh, R., and Saghaei, H., 2022. Design and simulation of high-quality factor all-optical demultiplexers based on two-dimensional photonic crystal. *Opt. Contin.*, **1**(7), pp. 1458–1473. DOI: 10.1364/OPTCON.460044
28. Liu, W., Zhang, L., and Zhang, F., 2022. Performance analysis of three-wavelength multi-channel photonic crystal filters of different sizes. *Crystals*, **12**(1), pp. 91–102. DOI: 10.3390/cryst12010091
29. Djavid, M., Dastjerdi, M.H.T., Philip, M.R., Choudhary, D., Pham, T.T., Khreishah, A., and Nguyen, H.P.T., 2018. Photonic crystal-based permutation switch for optical networks. *Photonic Netw. Commun.*, **35**, pp. 90–96. DOI: 10.1007/s11107-017-0719-7
30. Shmat'ko, A.A., Mizernik, V.N., Odarenko, E.N., Shevchenko, N.G., and Butenko, N.S., 2021. Narrow band filtering on the base of tunable magnetophotonic crystal. In: *2021 4th Int. Conf. on Advanced Information and Communication Technologies (AICT)*. Lviv, Ukraine, 21–25 Sept. 2021. P. 41–45. DOI: 10.1109/AICT52120.2021.9628910
31. Mohmoud, M.Y., Bassou, Gh., Taalbi, A., and Chekroun, Z.M., 2012. Optical channel drop filters based on photonic crystal ring resonators. *Opt. Commun.*, **285**(3), pp. 368–372. DOI: 10.1016/j.optcom.2011.09.068
32. Ma, Z., and Ogusu, K., 2011. Channel drop filters using photonic crystal Fabry-Perot resonators. *Opt. Commun.*, **284**(5), pp. 1192–1196. DOI: 10.1016/j.optcom.2010.10.050
33. Shmat'ko, A.A., Odarenko, E.N., Mizernik, V.N., and Shevchenko, N. G., 2020. Tunable angular spatial filter based on 1D magnetophotonic crystal. In: *2020 IEEE 15th Int. Conf. on Advanced Trends in Radioelectronics, Telecommunications and Computer Engineering (TCSET)*. Lviv-Slavske, Ukraine, 25–29 Febr. 2020. P. 207–212. DOI: 10.1109/TCSET49122.2020.235424
34. Jafari, R., Sahrai, M., Bozorgzadeh, F., Mohammadi-Asl, R., Ahmadi, D., and Movahednia, M., 2022. Narrow-band transmission filter based on 1D-PCs with a defect layer. *Appl. Opt.*, **61**(25), pp. 7463–7468. DOI: 10.1364/AO.452630
35. Zhao, X., Yang, Y., Wen, J., Chen, Z., Zhang, M., Fei, H., and Hao, Y., 2017. Tunable dual-channel filter based on the photonic crystal with air defects. *Appl. Opt.*, **56**(19), pp. 5463–5469. DOI: 10.1364/AO.56.005463
36. Gryga, M., Ciprian, D., Gembalova, L., and Hlubina, P., 2023. One-Dimensional Photonic Crystal with a Defect Layer Utilized as an Optical Filter in Narrow Linewidth LED-Based Sources. *Crystals*, **13**(1), 93. DOI: 10.3390/cryst13010093
37. Brown, B.M., Eastham, M.S.P., and Schmidt, K.M., 2013. *Periodic differential operators*. Operator theory: Advances and Applications. **230**. Basel: Springer. 216 p.

38. Shmat'ko, A.A., Mizernik, V.N., Odarenko, E.N., and Lysytsya, V.T., 2017. Dispersion Properties of TM and TE Modes of Gyrotropic Magnetophotonic Crystals. In: Vakhrushev, A.V. ed. *Theoretical foundations and applications of photonic crystals*. London: InTech, pp. 47–69. DOI: 10.5772/intechopen.71273
39. Shmat'ko, A.A., Odarenko, E.N., and Mizernik, V.N., 2023. Surface waves Fabry-Perot modes of the finite magnetophotonic crystal in Voigt configuration. *J. Electromagn. Waves Appl.*, **37**(6), pp. 827–851. DOI: 10.1080/09205071.2023.2212177
40. Arnaud, J.A., and Saleh, A.A.M., 1974. Guidance of surface waves by multilayer coatings. *Appl. Opt.*, **13**(1), pp. 2343–2345. DOI: 10.1364/AO.13.002343
41. Robertson, W.M., and May, M.S., 1999. Surface electromagnetic wave excitation on one-dimensional photonic band-gap arrays. *Appl. Phys. Lett.*, **74**, pp. 1800–1802. DOI: 10.1063/1.123090
42. Shmat'ko, A.A., Mizernik, V.N., and Odarenko, E.N., 2018. Surface and bulk modes of magnetophotonic crystals. In: *2018 14th Int. Conf. on Advanced Trends in Radioelectronics, Telecommunications and Computer Engineering (TCSET)*. Lviv-Slavske, Ukraine, 20–24 Febr. 2018. P. 436–440. DOI: 10.1109/TCSET.2018.8336235
43. Smolik, G.M., Descharmes, N., and Herzig, H.P., 2018. Toward Bloch Surface Wave-Assisted Spectroscopy in the Mid-Infrared Region. *ACS Photonics*, **5**(4), pp. 1164–1170. DOI: 10.1021/acsp Photonics.7b01315
44. Tuz, V.R., Fedorin, I.V., Fesenko, V.I., 2017. Bi-hyperbolic isofrequency surface in a magnetic-semiconductor superlattice. *Opt. Lett.*, **42** (21), pp. 4561–4564. DOI: 10.1364/OL.42.004561

Received 15.08.2023

О.О. Шматько<sup>1</sup>, Є.М. Одаренко<sup>2</sup>

<sup>1</sup> Харківський національний університет імені В.Н. Каразіна  
майдан Свободи, 4, м. Харків, 61022, Україна

<sup>2</sup> Харківський національний університет радіоелектроніки  
просп. Науки, 14, м. Харків, 61166, Україна

#### ВУЗЬКОСМУГОВИЙ ФІЛЬТР НА ОСНОВІ МАГНІТОФОТОННОГО КРИСТАЛА, ЩО МІСТИТЬ ШАРИ З ГІПЕРБОЛІЧНИМ ЗАКОНОМ ДИСПЕРСІЇ

**Предмет і мета роботи.** Вузькосмугові фільтри є одними з основних компонентів сучасних систем зв'язку, спектроскопії, високочутливих сенсорів тощо. Фотонно-кристалічні структури відкривають широкі можливості для створення компактних вузькосмугових фільтрів оптичного та терагерцового діапазонів. Налаштування спектральних характеристик фотонно-кристалічних фільтрів зазвичай здійснюється шляхом введення в їхню структуру елементів, чутливих до зовнішніх електричних і магнітних полів. Метою даної роботи є дослідження електродинамічних характеристик одновимірного магнітофотонного кристала з шарами, які характеризуються гіперболічним законом дисперсії, та створення на цій основі багатоканального вузькосмугового фільтра.

**Методи та методологія.** У рамках методу Флоке–Блоха з використанням фундаментальних розв'язків рівняння Хілла отримано дисперсійне рівняння для нескінченного магнітофотонного кристала. Для отримання аналітичного виразу для коефіцієнта пропускання використано метод матриці передачі.

**Результати.** Проаналізовано дисперсійну діаграму одновимірного магнітофотонного кристала для випадку, коли один із шарів на періоді структури характеризується гіперболічним законом дисперсії. Знайдено області існування поверхневих хвильових режимів у таких шарах періодичної структури за умови нормального падіння хвилі на скінченний магнітофотонний кристал. Частотні залежності коефіцієнта пропускання характеризуються набором високодобротних резонансних піків, що є обумовленими резонансами Фабрі–Перо в скінченній періодичній структурі.

**Висновки.** Розглянуто застосування скінченного одновимірного магнітофотонного кристала для оптичної багатоканальної фільтрації та формування частотної гребінки. Отримано дисперсійне рівняння та вираз для коефіцієнта пропускання в рамках методу Флоке–Блоха та матриці передачі. Показано можливість реалізації мод поверхневих хвиль у шарах періодичної структури, які характеризуються гіперболічним законом дисперсії, за умови нормального падіння хвилі на магнітофотонний кристал. Спектральна характеристика фільтра містить вузькосмугові піки з високим коефіцієнтом пропускання. Збільшення кількості періодів структури приводить до формування частотної гребінки, яка може бути використаною в метрології та сучасних оптичних комунікаційних системах.

**Ключові слова:** магнітофотонний кристал, гіперболічні середовища, вузькосмугова фільтрація, частотна гребінка, дисперсійні характеристики, режими поверхневих хвиль.